Biochem. J. (1977) **165**, 207–225
Printed in Great Britain

The Combining Site of the Dinitrophenyl-Binding Immunoglobulin A Myeloma Protein MOPC 315

By STEVEN K. DOWER,* SIMON WAIN-HOBSON,* PETER GETTINS,* DAVID GIVOL,† W. ROLAND C. JACKSON,* STEPHEN J. PERKINS,‡ CHRISTOPHER A. SUNDERLAND,* BRIAN J. SUTTON,* CAROLYN E. WRIGHT‡ and RAYMOND A. DWEK*

**Department of Biochemistry, University of Oxford, South Parks Road, Oxford OX1 3QU, U.K.,*
†*Department of Chemical Immunology, Weizmann Institute for Science, Rehovot, Israel, and*
‡*Laboratory of Molecular Biophysics, Department of Zoology, University of Oxford, South Parks Road, Oxford OX1 3PS, U.K.*

(*Received* 26 *October* 1976)

Magnetic-resonance techniques are used to refine the model of the combining site of the Fv fragment of the dinitrophenyl-binding mouse myeloma protein MOPC 315 constructed by Padlan, Davies, Pecht, Givol & Wright (1976) (*Cold Spring Harbor Symp. Quant. Biol.* **41**, in the press). Light-absorption studies indicate a dinitrophenyl–tryptophan interaction in the Fv fragment of the type occurring in free solution. The Dnp-aspartate–tryptophan complex is therefore used as a starting point for the n.m.r. (nuclear-magnetic-resonance) analysis of the dinitrophenyl–Fv fragment interaction. Ring-current calculations are used to determine the geometry of the complex. The specificity of complex-formation between dinitrophenyl and tryptophan is confirmed by the lack of ring-current shifts of the dinitrophenyl resonances when tryptophan is replaced by any other aromatic amino acid. Proton n.m.r. difference spectra (at 270 MHz), resulting from the addition of a variety of haptens to the Fv fragment, show that the combining site is highly aromatic in nature. Calculations on the basis of ring-current shifts define the geometry of the combining site, which involves a dinitrophenyl ring in van der Waals contact with four aromatic amino acid residues on the protein. The observation of a nuclear Overhauser effect on the $H_{(3)}$ resonance of the dinitrophenyl ring provides additional constraints on the relative geometry of the $H_{(3)}$ proton and an aromatic amino acid residue on the Fv fragment. The specificity of the Fv fragment for dinitrophenyl ligands arises from a stacking interaction of the dinitrophenyl ring with tryptophan-93_L, in an 'aromatic box' of essentially tryptophan-93_L, phenylalanine-34_H and tyrosine-34_L; asparagine-36_L and tyrosine-34_L also contribute by forming hydrogen bonds with the nitro groups on the dinitrophenyl ring. The n.m.r. results also confirm that the antibody–hapten reaction may be visualized as a single encounter step. An Appendix shows the method of calculation of ring currents for the four aromatic amino acids and their use in calculating structures.

X-ray-crystallographic studies have shown that the basic antibody structural unit is the immunoglobulin fold (Poljak *et al.*, 1973; Schiffer *et al.*, 1973; Amzel *et al.*, 1974; Epp *et al.*, 1974; Segal *et al.*, 1974; Poljak, 1975; Davies *et al.*, 1975*a*,*b*). This consists of two layers of anti-parallel β-pleated sheets. One of these layers has three hydrogen-bonded anti-parallel strands and the other layer has four. The intradomain disulphide bond is located at the centre of each domain and connects the middle section of the three-chain layer with a strand in the other layer.

The concept of the immunoglobulin fold as the basic structural unit has led to the suggestion that the variable region may be regarded as consisting of a rigid framework, to which the hypervariable regions or loops are attached. Since the structures of several immunoglobulin fragments are known (Poljak *et al.*, 1974; Poljak, 1975; Davies *et al.*, 1975*a*,*b*), it is feasible to construct, by model building, the hypervariable regions and thus the binding sites of different immunoglobulins from their amino acid sequences.

Thus Poljak *et al.* (1974) suggested that the crystal structure of the Fab′ New fragment could be used as a basic structural framework to predict the structure of the combining site of the dinitrophenyl-binding mouse myeloma IgA§ produced by MOPC 315. A more detailed model-building study of this combining site was carried out by Padlan *et al.* (1976) using mainly the co-ordinates of protein

§Abbreviations: IgA, immunoglobulin A; Fv fragment, variable region of heavy and light chains; n.m.r., nuclear magnetic resonance; e.s.r., electron spin resonance; Dnp and Tnp, di- and tri-nitrophenyl; Pipes, 1,4-piperazine-diethanesulphonic acid.

McPC 603, but additionally most of the available three-dimensional data from other immunoglobulin structures. The predicted model is in accordance with the results of affinity-labelling studies (Givol, 1974), but such agreement derives from coarse rather than fine details of the model. The combining site of the Fv fragment (Hochman *et al.*, 1973) of protein MOPC 315 may be further characterized by the use of n.m.r. and e.s.r.

By concentrating mainly on the combining site many problems normally encountered in a complete structural determination of the whole fragment would be avoided.

The prediction by model building of the combining site of protein MOPC 315 was of enormous help to the n.m.r. structural studies, for it provided a structure which could be regarded as a first approximation, and then altered or refined to make it compatible with the large amount of physical data that had been accumulated. In particular, since n.m.r. can provide details at atomic resolution, often to within 0.1 nm, this would allow the relative orientations of the amino acids in the combining site to be determined.

Our previous papers (Dwek *et al.*, 1975*a*,*b*) have shown that the combining site of the Fv fragment is highly aromatic in nature and has considerable structural rigidity. The high density of aromatic amino acid residues results in ring-current shifts of resonances both from the Fv fragment itself and from the hapten contained within the site. The present paper is concerned with obtaining geometrical information from ring-current shifts on resonances of bound Dnp-haptens. With the results from the interaction between dinitrophenyl derivatives and tryptophan, we propose that, in the combining site of the Fv fragment, the dinitrophenyl ring forms a stacked complex with a tryptophan residue and is also in contact with at least three other aromatic amino acid residues. Conclusions from spectroscopic data in conjunction with the model of the combining site lead to the assignment and positioning of aromatic amino acid residues relative to the hapten, and to an understanding of the specificity of protein MOPC 315 for dinitrophenyl ligands.

Materials and Methods

Preparation of solutions of protein MOPC 315 Fv fragment

The Fv fragment of the mouse myeloma IgA protein MOPC 315 was prepared as described by Inbar *et al.* (1972). Samples for the n.m.r. studies were prepared by dissolving the freeze-dried protein in ^2H_2O (Ryvan Chemicals, Hedge End, Southampton; 99.8% ^2H_2O). The pH* (pH uncorrected for the ^2H isotope effect) was adjusted with dilute solutions of NaO^2H or ^2HCl. All solutions contained 0.15 M-NaCl.

Samples for the absorption difference spectroscopy and fluorescence studies were prepared by dissolving the freeze-dried protein in distilled water. The pH was adjusted with dilute HCl or NaOH solutions. All solutions contained 0.15 M-NaCl.

Preparation of hapten and tryptophan solutions

Dnp-L-aspartic acid, ε-Dnp-L-lysine and Dnp-glycine were purchased from BDH Chemicals, Poole, Dorset, U.K. Dinitrophenol was purchased from Hopkin and Williams, Romford, Essex, U.K., and purified by recrystallization from ethyl acetate. Dinitrobenzene was purchased from BDH. Dnp-aminoethyl phosphate and Dnp-aminomethylphosphonate were prepared as described in Wain-Hobson *et al.* (1977). L-Tryptophan was purchased from Fisons, Loughborough, Leics., U.K.

The solutions were prepared by dissolving haptens or L-tryptophan in ^2H_2O or distilled water, as described above.

High-resolution n.m.r. studies

Spectra were recorded at 270 MHz on a Bruker spectrometer as described in Dwek *et al.* (1975*a*) and at 90 MHz on a Bruker spectrometer operating in the Fourier-transform mode with a Bruker BNC-12 data system. Spectra were recorded with a probe temperature of 30±1°C.

Fluorescence studies

Fluorescence spectra were recorded on a Perkin–Elmer/Hitachi MPF-2A spectrofluorimeter, as described by Dwek *et al.* (1976).

Absorption difference spectroscopy

Absorption spectra were recorded on a Cary 17 recording spectrophotometer, with Hellma QS tandem cells.

Analysis of binding data from n.m.r. studies

Model studies. The binding of hapten to tryptophan cannot be analysed on a simple 1:1 basis, but is consistent with the following model:

$$\text{Hapten} + \text{Trp} \overset{K_{D1}}{\rightleftharpoons} \text{hapten–Trp} \quad (1)$$

$$\text{Hapten–Trp} + \text{Trp} \overset{K_{D2}}{\rightleftharpoons} \text{Trp–hapten–Trp} \quad (2)$$

Although the haptens self-associate, the binding is sufficiently weak ($K_D > 1$ M for Dnp-aspartate) for it not to affect the analysis.

The binding of hapten to tryptophan results in changes of chemical shift, $\Delta\delta_{obs.}$, of the hapten and tryptophan resonances. Under conditions of fast exchange:

$$\Delta\delta_{obs.} = X_{bin.}\,\Delta\delta_{bin.} + X_{ter.}\,\Delta\delta_{ter.} \quad (3)$$

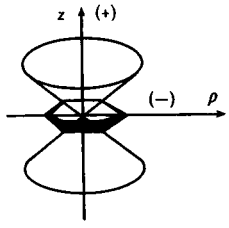

Fig. 1. *Shielding envelope for the ring-current shifts from a benzene ring*

The cone separates the shielding (+, upfield-shifted) and deshielding (−, downfield-shifted) regions. The z direction is along the hexagonal axis of the benzene ring, and ρ is the direction in the plane of the carbon atoms.

where $X_{bin.}$ and $X_{ter.}$ are the fractions of hapten or tryptophan bound in the binary and ternary complexes respectively, and $\Delta\delta_{bin.}$ and $\Delta\delta_{ter.}$ are the corresponding fully bound shifts. A simple iterative procedure was used to calculate theoretical curves for a range of values of K_D and fully bound shifts. These curves were then compared with the experimental data.

Antibody-binding studies. Hapten binding to antibody is sufficiently tight to satisfy the relationship $[\text{hapten}],[\text{protein}] \gg K_D$. Hence $[\text{hapten}]_{bound} = [\text{protein}]_{total}$ when $[\text{hapten}]_{total} > [\text{protein}]_{total}$. Thus:

$$\frac{\Delta\delta_{obs.}}{\Delta\delta} = \frac{[\text{protein}]_{total}}{[\text{hapten}]_{total}}$$

and a plot of $\Delta\delta_{obs.}$ against $1/[\text{hapten}]_{total}$ will yield the fully bound hapten chemical shift.

Use of ring-current shifts to calculate structures

The circulation of the delocalized π electrons of the aromatic rings gives rise to secondary fields when the aromatic rings are placed in a magnetic field. Nuclei located above or below the aromatic ring are upfield-shifted as they are shielded. Nuclei in the plane of the ring are deshielded, and thus resonate at lower field (Dwek, 1973) (Fig. 1). The magnitude, B, of these shifts may be approximated by the dipole equation:

$$B \propto \frac{(3\cos^2\theta - 1)}{r^3}$$

where r is the distance of the nucleus from the ring centre, and θ is the angle between r and the direction of the applied field. The inverse power–distance term indicates that the magnitude of the effect falls off rapidly with distance.

Two methods are used to calculate structures from ring-current shifts. In the first, a FORTRAN program RSEARCH is used to test a large number of structures against the Johnson–Bovey (1958) equation. The second approach is a manual method, by use of contour maps constructed from ring-current tables. Further details are given in the Appendix. Whereas the computer approach can readily test all possible geometrical solutions for a two-ring interaction, the introduction of three more rings makes the manual method desirable in view of the much greater number of permutations that would otherwise need to be tested.

Results and Discussion

Interaction of tryptophan with dinitrophenyl ligands

Little & Eisen (1967) have shown that the changes in u.v.-absorbance spectra of di- and tri-nitrophenyl ligands on binding to anti-dinitrophenyl and anti-trinitrophenyl antibodies can be quantitatively reproduced when the same haptens were mixed with L-tryptophan in various solvents, but not with other amino acids. The finding by Eisen *et al.* (1968) that similar spectral shifts for tri- and di-nitrophenyl ligands were observed when bound to the mouse myeloma protein MOPC 315 suggests interaction of these ligands with a tryptophan residue. Furthermore large negative enthalpies (Johnston *et al.*, 1974) and circular-dichroic difference spectra (Rockey *et al.*, 1972; Freed *et al.*, 1976) associated with di- or trinitrophenyl binding to protein MOPC 315 reinforce the suggestion that a hapten–tryptophan complex could well be a major factor in the specificity of protein MOPC 315 for polynitrated phenols. It is important, therefore, to establish the specific structural basis for the observed spectral changes. N.m.r. can provide this information, since the changes in chemical shifts caused by the ring-current effects of aromatic molecules in close proximity are related to the geometry of the system (Dwek, 1973).

Fig. 2 shows the 270MHz proton spectrum of a mixture of Dnp-aspartate and L-tryptophan in ^2H_2O at pH6.0. The assignment of resonances to individual protons is shown above each peak or multiplet.

The binding of Dnp-aspartate to L-tryptophan was analysed by carrying out titrations in which the chemical shifts of one of the components (present at constant concentration) was measured as a function of the concentration of the other. All resonances shift upfield, the values of the shifts being different for each proton. Two such titrations are shown in Figs. 3(*a*) and 3(*b*). It is not possible to explain the behaviour in terms of a single dissociation constant, and, in addition to the binary complex, a complex of the type Trp-Dnp-Trp has to be considered. A good fit to the data is obtained by using the model as defined in eqns. (1) and (2), with the parameters $K_{D1} = 35$–50mM, $K_{D2} = 140$–200mM (with $K_{D2} = 4K_{D1}$) and the values of the fully bound shifts as given in Table 1. In the titration in Fig. 3(*a*), formation of

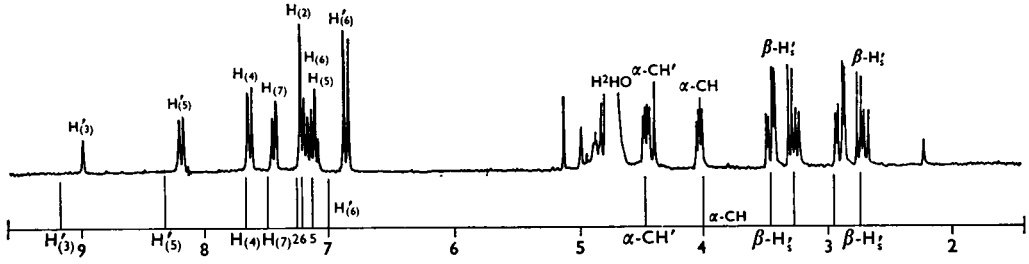

Fig. 2. *Proton spectrum at 270 MHz of a mixture of Dnp-aspartate and tryptophan*
The shifts on complex-formation are all upfield for the aromatic protons. The shifts of the protons in the free compounds are indicated. Conditions were 10mM-Trp, 10mM-Dnp-aspartate, 150mM-NaCl, pH6.0, and $T = 303$K.

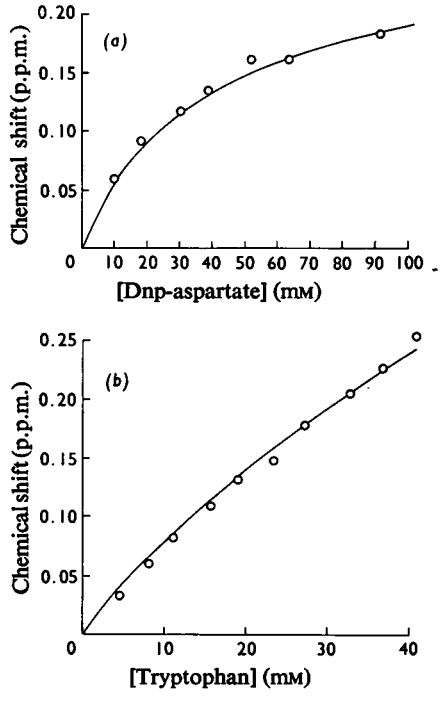

Fig. 3. *Titration of the chemical shifts of (a) the $H_{(7)}$ proton of tryptophan (4mM) with Dnp-aspartate and (b) the $H_{(3)}$ proton of Dnp-aspartate (4.14mM) with tryptophan*
Conditions for both titrations were pH6.0, 0.15M-NaCl and $T = 303$K. The continuous lines are theoretical fits to the data, assuming $K_{D1} = 40$mM, $K_{D2} = 160$mM [cf. eqns. (1) and (2)] and fully bound shifts of 0.26 and 0.37p.p.m. for the tryptophan $H_{(7)}$ proton and Dnp-aspartate $H_{(3)}$ proton respectively in the binary complex, and 0.74p.p.m. for the Dnp-aspartate $H_{(3)}$ proton in the ternary complex.

the ternary complex is insignificant, since the tryptophan concentration is low throughout the titration; hence the fully bound shifts for the tryptophan protons in the binary complex can be estimated accurately. By contrast, there is significant formation of the ternary complex in Fig. 3(*b*), which makes it difficult to estimate the fully bound shifts on the dinitrophenyl protons. The values of these shifts given in Table 1 must be regarded as only approximate. However, the shift ratios are constant throughout the titration, and it is these ratios, rather than the absolute values, that are used initially in calculating the structure of the binary complex.

Interaction of tryptophan with Dnp-OH and Tnp-aminomethyl phosphonate

The addition of either of these ligands to tryptophan solutions results in upfield chemical shifts, which are quantitatively very similar to those observed in solutions containing Dnp-aspartate.

Specificity of complex-formation

The specific interaction between tryptophan and dinitrophenyl ligands is illustrated by replacing tryptophan by one of the other aromatic amino acids. In titrations similar to those in Fig. 3, but at 90 MHz, no upfield changes in chemical shift were observed. Furthermore no chemical-shift changes were observed in solutions containing tryptophan (10mM) in which the Dnp-aspartate was replaced by either tyrosine (10mM) or phenylalanine (10mM). All the findings reported here agree with the conclusions of Little & Eisen (1967).

Structure of the Dnp-aspartate–tryptophan complex

The set of fully bound chemical shifts of the protons of the Dnp-aspartate–tryptophan complex provides the basis for determining its structure, if it is assumed that the shift changes originate only from ring-current interactions. All the observed shift changes of the protons in the aromatic rings are upfield, which indicates a stacking interaction. Since the closest distance of approach of two rings is expected to be 0.33nm (Hanson, 1964), a physically reasonable starting point for the calculation of expected ring-

Table 1. *Experimental and calculated bound shifts (p.p.m.) and shift ratios of the aromatic protons of the Dnp-aspartate–L-tryptophan complex*

The experimental shift(s) are those determined for the fully bound complex at pH 6.0 and $T = 303$ K. The calculated shifts were derived from the Johnson–Bovey (1958) equation (see the Appendix) for the structure obtained from the computer program RSEARCH, and shown in Fig. 6. The shifts are the changes in position of the protons from those in the free compound, and the shift ratios for both compounds are quoted with respect to their $H_{(6)}$ protons.

	Shift		Shift ratio	
Proton	Experimental	Calculated	Experimental	Calculated
Dnp-Asp $H_{(3)}$	0.35–0.55	0.71	1.98	1.86
Dnp-Asp $H_{(5)}$	0.22–0.35	0.43	1.26	1.13
Dnp-Asp $H_{(6)}$	0.17–0.27	0.38	1.00	1.00
Trp $H_{(2)}$	0.19	0.10	0.96	0.37
Trp $H_{(4)}$	0.23	0.29	1.21	1.07
Trp $H_{(5)}$	0.18	0.23	0.92	0.85
Trp $H_{(6)}$	0.19	0.27	1.00	1.00
Trp $H_{(7)}$	0.26	0.53	1.34	1.96

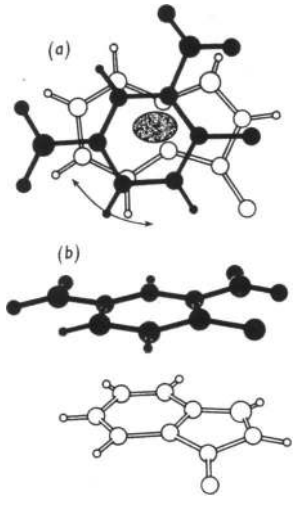

Fig. 4. *Structure of the Dnp-aspartate and tryptophan complex*

The two views are obtained from a computer search of the possible structures, with a separation between the two aromatic rings of 0.33 nm, which give calculated ring-current shifts in agreement with those obtained experimentally. The shifts are calculated by the Johnson–Bovey (1958) equation, modified to take into account the aromatic nature of the indole ring. The two views represent (*a*) a vertical view down the *z*-axis and (*b*) that vertical view rotated 30° about the *z*-axis and 60° about the *x*-axis. The ellipse and the arrows indicate the extent of the family of solutions, of which the structure shown is a member.

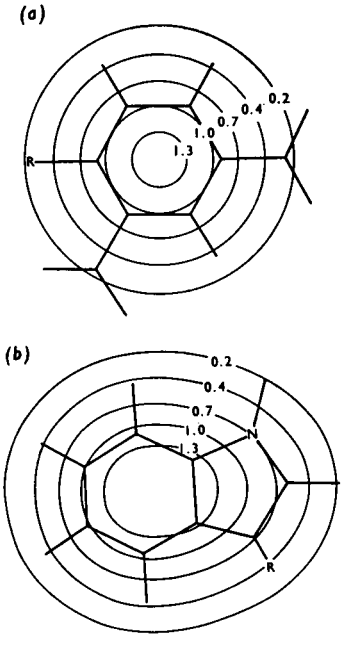

Fig. 5. *Contour maps of the ring-current shifts relevant to the Dnp-aspartate–tryptophan complex*

The contour maps are illustrated for the shifts on a nucleus 0.33 nm above the plane of the ring. (*a*) Dinitrophenyl ring, assuming that the nitro groups have no effect on the magnitude of the ring current. (*b*) Tryptophan calculated from the modified Johnson–Bovey (1958) treatment as discussed in the Appendix.

current shifts is with the planes parallel and separated by this distance.

Because the absolute magnitudes of the shift changes of the Dnp-aspartate resonances are not known exactly, as discussed above, the ratios of the observed shift changes are used for the initial computer search. Two distinct sets of solutions are found. One has the centre of the dinitrophenyl ring positioned over the centre of the benzene ring of the

tryptophan, and the other, shown in Fig. 4, has it positioned closer to the pyrrole ring. Further searches, using interplanar distances of 0.34 and 0.35nm, as reported for a tryptophan–picrate complex (Gartland *et al.*, 1974), give the same two sets of solutions. One of these sets can be ruled out, since structures with the centre of the dinitrophenyl ring positioned over the centre of the benzene ring of the tryptophan are not compatible with the absolute magnitudes or shift ratios of the tryptophan protons, whereas structures of the type shown in Fig. 4 are consistent with the data. An equivalent set of solutions, related by a 180° rotation, is possible owing to the assumed symmetry of the indole ring. Fig. 4 also shows the range of positions of the centre of the dinitrophenyl ring and of rotations about the centre, contained in this set of structures of the binary complex. The contour diagrams of the ring-current shifts of dinitrophenyl and tryptophan for an interplanar separation of 0.33nm used to determine the complex structure are shown in Fig. 5.

Hapten difference spectra and the aromatic nature of the combining site

The 270MHz proton n.m.r. difference spectra resulting from the addition of a variety of haptens to the Fv fragment are shown in Fig. 6.

The intensities of these difference spectra represent only 2–3% of the total intensity of the Fv fragment spectrum, indicating that very few proton resonances are perturbed on hapten binding. This shows that any conformational changes on hapten binding are very small and are limited to the immediate vicinity of the combining site.

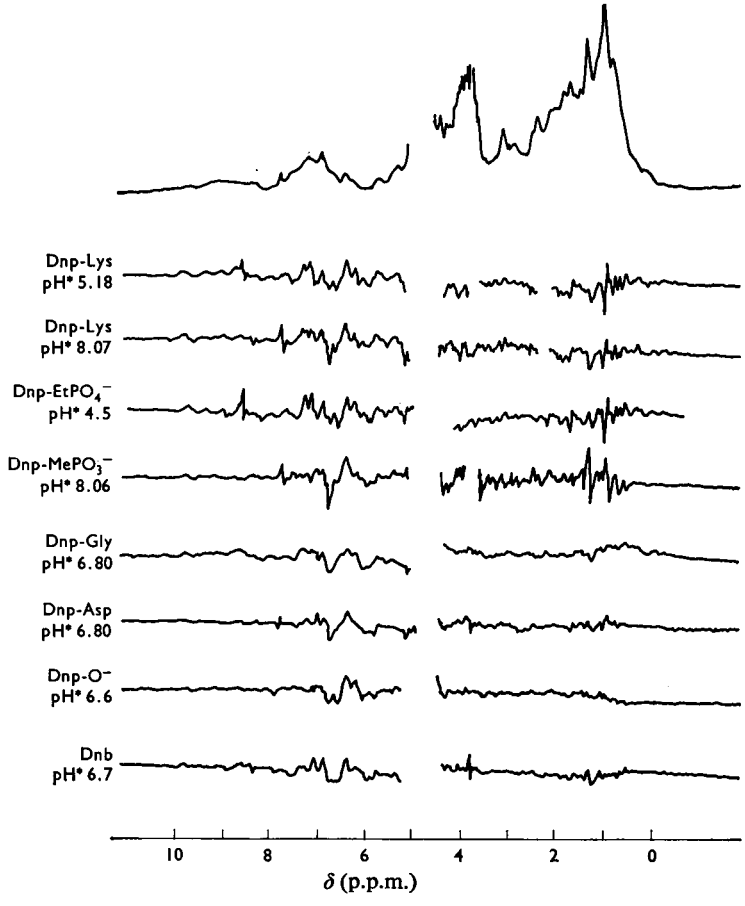

Fig. 6. *Proton-magnetic-resonance difference spectra at 270MHz resulting from the binding of various haptens to the Fv fragment*

The haptens and the pH of each experiment are indicated, and all measurements were made at $T=303$K. The concentration of the Fv fragment and the haptens are both about 1.2mM each time. The difference-spectra intensities are all 2× the intensity of the Fv fragment spectrum. Dnp-$EtPO_4^-$, Dnp-aminoethyl phosphate; Dnp-$MePO_3^-$, Dnp-aminomethylphosphonate; Dnb, dinitrobenzene. pH* is pH uncorrected for ^2H isotope effect.

An important feature of these difference spectra is that the protons consistently perturbed are almost entirely aromatic. By using the intensity of the histidine $C_{(2)}$ protons as an internal marker, it is possible to estimate that about 10–12 protons from aromatic amino acid residues in the Fv fragment are perturbed on hapten binding. This means that only about four aromatic amino acids can be in contact with the hapten.

In a previous paper (Dwek *et al.*, 1975*a*) the difference spectrum obtained in the presence of a spin-labelled hapten was reported. The spin-label hapten broadens resonances of protons close to it in space, hence resonances that appear in the difference spectrum are assigned to groups in or near the combining site. This spin-labelled difference spectrum, which contains resonances from residues within about 1–1.2nm of the nitroxide, does not reveal any very unusual shifts for methyl groups (Dwek *et al.*, 1975*a*). We conclude that none of the six amino acids that contain methyl groups is in the vicinity of the hapten, and that any methyl groups within the spin-label broadening sphere experience only very minimal interactions with any aromatic residues, i.e. they do not approach closer than about 0.4nm.

The conclusion that there are no aliphatic residues containing methyl groups in the combining site is important, since in the model of the Fv fragment

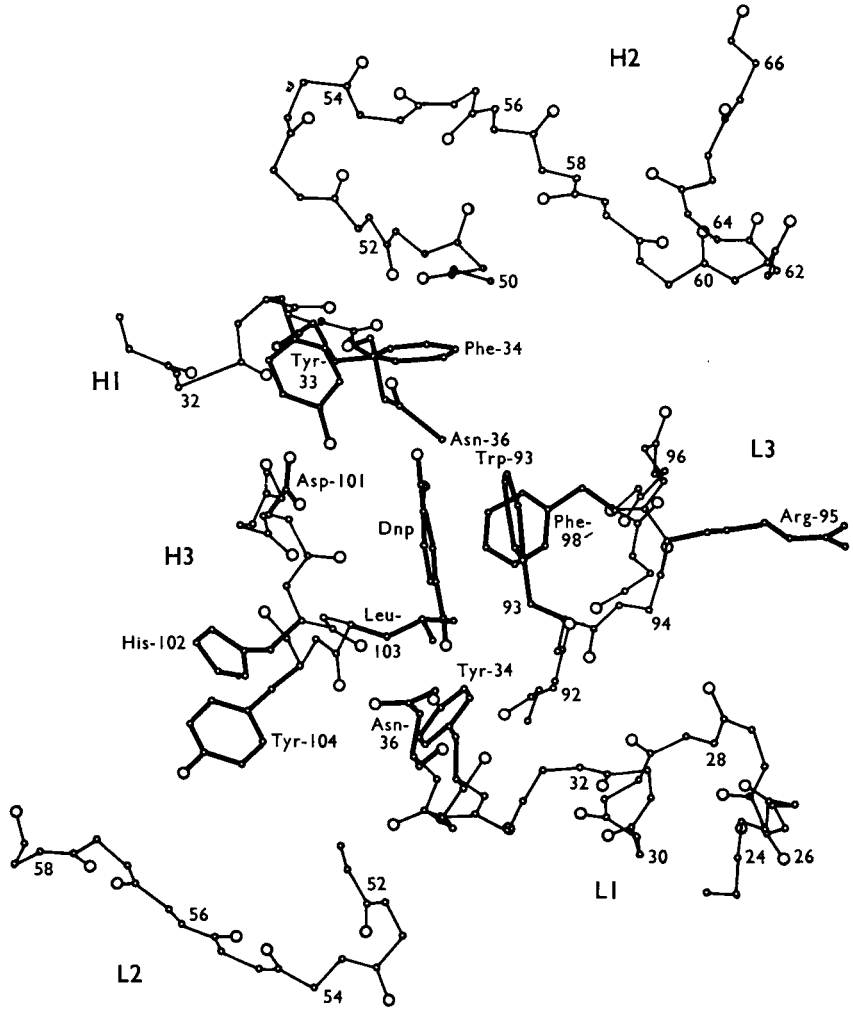

Fig. 7. *Predicted combining site of protein MOPC* 315

This is obtained from the co-ordinates of Padlan *et al.* (1976), which have been very kindly made available to us before publication. The hypervariable loops of the heavy (H) and light (L) chains, and the hapten position relative to the two chains, are indicated.

postulated by Padlan *et al.* (1976) leucine-103_H is given as a contact residue. A picture of the predicted combining site is shown in Fig. 7. However, these authors do point out that, if, in protein MOPC 315, the third hypervariable segment of the heavy chain containing this residue is built to have the same configuration as in the Fab' New fragment (Poljak *et al.*, 1974), then leucine-103 would project out of the combining site and tyrosine-104_H would project into the site.

The revised model would therefore have a remarkable concentration of aromatic residues in the site with the consequences that (1) the shifts on the hapten proton resonances arising from the ring currents of those residues allow the relative positioning of the hapten ring and neighbouring aromatic amino acid residues, and (2) the aromatic amino acids in the combining site will experience ring-current shifts from one another. This will lead to some unusual chemical shifts for aromatic proton resonances from the Fv fragment. This is indeed the case, for there are several resonances centred around 6.3 p.p.m. in the Fv fragment spectrum (Fig. 6), which are shifted at least 1 p.p.m. upfield from the normal random-coil positions and which are affected on hapten binding. The difference spectra shown here thus provide evidence that the structure of the Fv fragment predicted by Padlan *et al.* (1976) is essentially correct.

Comparison of the aromatic region of the difference spectra shows that they are remarkably similar

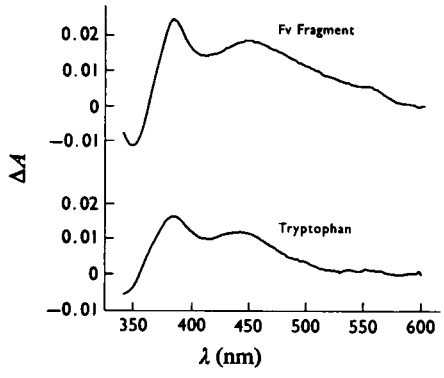

Fig. 8. *Comparison of the difference absorption spectra of Dnp-aspartate on interaction with either the Fv fragment or tryptophan*

Conditions were: Dnp-aspartate, 70μM; Fv fragment, 40μM; Trp, 20mM; pH 6.8; Pipes buffer, 40mM; NaCl, 0.15M. T=298K.

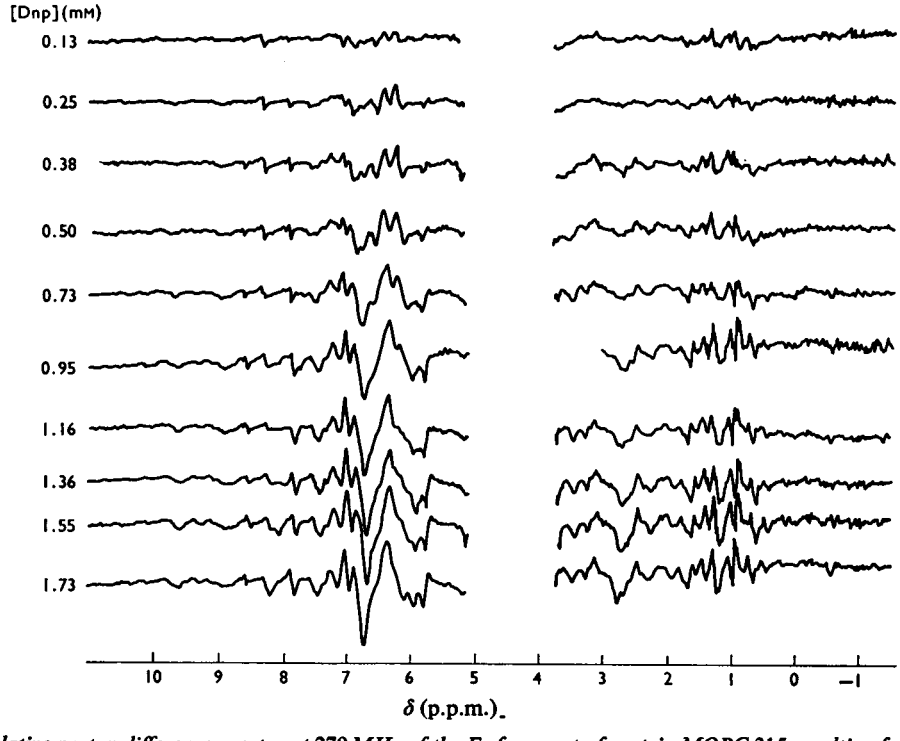

Fig. 9. *Cumulative proton difference spectra at 270 MHz of the Fv fragment of protein MOPC 315 resulting from addition of Dnp-aspartate at pH 6.9 and T=303 K in 0.15M-NaCl*

The differences are obtained from the initial spectrum, as described in text.

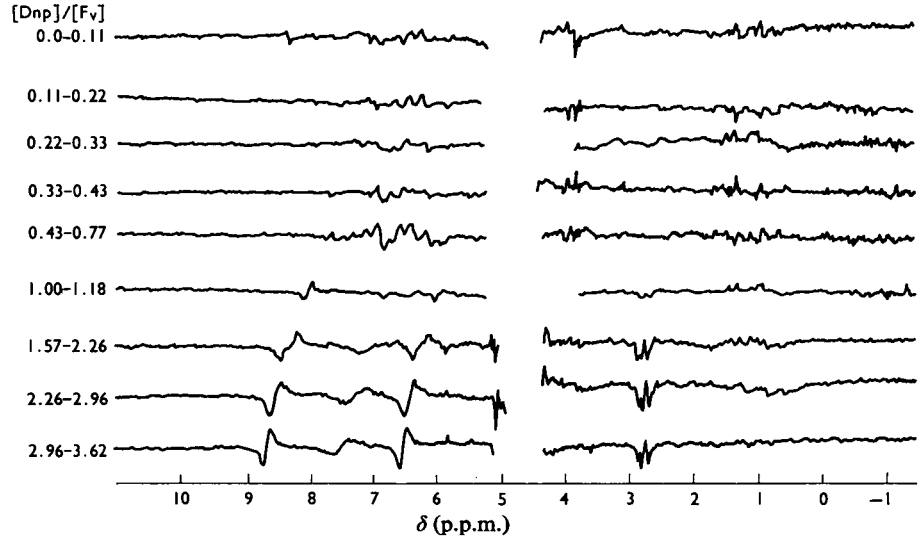

Fig. 10. *Serial difference spectra at 270 MHz of the Fv fragment of protein MOPC 315 resulting from addition of Dnp-aspartate at pH 6.9 and T = 303 K in 0.15 M-NaCl*

These difference spectra are between successive additions of hapten, and the ratios of Dnp-aspartate to Fv fragment are indicated each time. Note that after the ratio exceeds 1:1 only the hapten resonances continue to titrate.

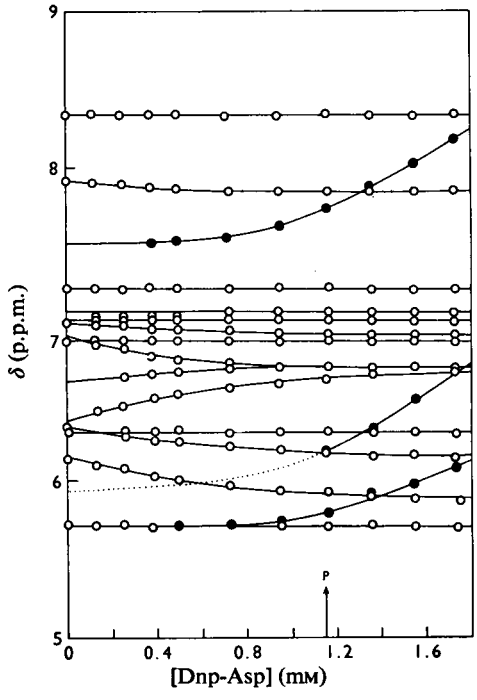

Fig. 11. *Summary of chemical-shift titrations at 270 MHz of the aromatic region of solutions of the Fv fragment and various amounts of Dnp-aspartate at pH 6.9 and T = 303 K in 0.15 M-NaCl*

The protein concentration is indicated by the letter P. The dotted line is extrapolated on the basis of the binding constant of approx. 20 μM determined from this titration.

in overall pattern, indicating that the same residues are perturbed by all haptens. The differences between the spectra reflect the interactions of the hapten side chains with the Fv fragment.

Binding of Dnp-aspartate to the Fv fragment

Fluorescence and absorption difference-spectroscopy studies. The binding of Dnp-aspartate to the Fv fragment was studied by observing the quenching of protein fluorescence as a function of the concentration of Dnp-aspartate. At pH 5.5 in Pipes/0.15 M-NaCl buffer and at 25°C the limiting fluorescence quenching is 0.45, and the dissociation constant is 17 μM.

Fig. 8 shows the change in the absorption spectrum of Dnp-aspartate in the presence of the Fv fragment and tryptophan. The similarity of these two difference spectra strongly suggests that a tryptophan residue in the combining site of the Fv fragment interacts with the dinitrophenyl group of the Dnp-aspartate (Eisen *et al.*, 1968). In the n.m.r. studies with tryptophan and Dnp-aspartate, it was shown that the explanation for this is a close stacking interaction of the tryptophan and dinitrophenyl rings.

High-resolution proton n.m.r. studies. The addition of Dnp-aspartate to the Fv fragment results in changes in the chemical shifts of the proton resonances of both hapten and protein. These are shown in Fig. 9, which illustrates the 270 MHz proton cumulative difference spectra (obtained by subtracting each spectrum from the initial one) resulting from successive additions of hapten. The use of serial difference spectra (Fig. 10) illustrates that, after the ratio of

Table 2. *Chemical shifts (δ_0) and the change in chemical shift ($\Delta\delta$) of resonances perturbed on binding of Dnp-aspartate to fraction Fv from protein MOPC* 315 *at pH* 6.9

Measurements are made at 270 MHz and $T = 303$ K and in the presence of 0.15 M-NaCl. Shifts were measured from the sodium salt of 3-(trimethylsilyl)propanesulphonic acid as an external standard. − denotes a downfield shift change; + denotes an upfield shift change.

Hapten resonances	δ_0 (p.p.m.)	$\Delta\delta$ (p.p.m.)	No. of protons
$H_{(3)}$	9.18	+1.68	1
$H_{(5)}$	8.36	+2.3	1
$H_{(6)}$	7.04	+1.31	1
$-CH_2-$	2.76	+0.1	
(Complex pattern with three main peaks)	2.91	+0.2	2
	2.99	+0.2	
–CH–		Not observable	
Protein resonances			
5.9 His $C_{(2)}$	7.82	+0.06	1
—	7.00	Broadens out	~2
5.9 His $C_{(4)}$	6.95	+0.07	1
—	6.90	+0.19	1
—	6.62	−0.08	1
—	6.37	−0.29	2
	6.33	+0.17	⩽2
	6.16	+0.25	2
Peak decreases as hapten is added	7.20		~2
Peak increases as hapten is added	7.42	Poss.: 0.22	2

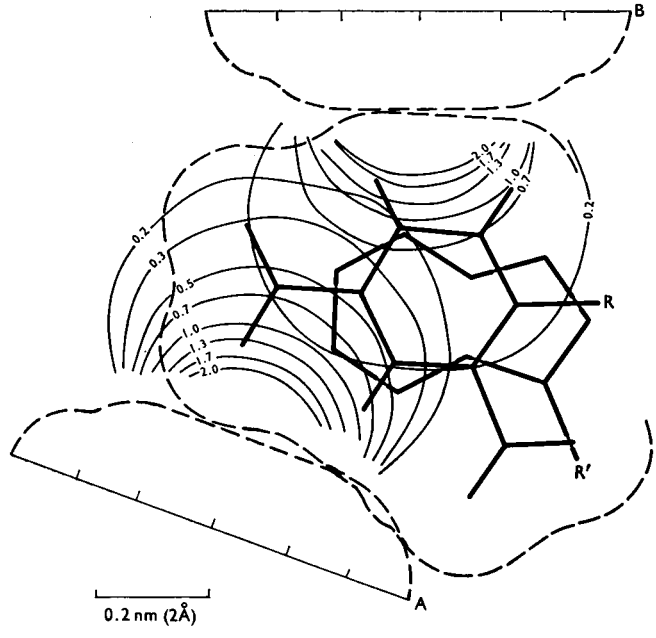

Fig. 12. *Relative geometry of aromatic rings around the dinitrophenyl ring in the combining site of protein MOPC* 315
The geometry is calculated on the basis of ring-current interactions on the hapten protons, assuming that the dinitrophenyl and tryptophan interaction is as shown in Fig. 4, but with one of the rings rotated through 180°. The van der Waals surfaces of the dinitrophenyl ring and of the two perpendicular aromatic rings labelled A and B are indicated. The perpendicular contour maps give some idea as to the possible movement of these rings which can still result in values of the ring-current shifts within experimental error. R and R′ represent the side chains of the dinitrophenyl and tryptophan rings. In the text it is argued that the tryptophan residue points back into the site.

hapten/Fv fragment exceeds 1:1, only the hapten resonances continue to shift, the actual position of each of these resonances representing the weighted mean of that of the free hapten and that when bound to the Fv fragment. The chemical-shift changes of the resonances in the aromatic region are shown in Fig. 11 and are summarized in Table 2.

The most notable feature of Table 2 is the extremely large upfield chemical shifts experienced by the dinitrophenyl protons. Of the proton resonances, apart from these assigned to histidine-97_L (pK_a 5.9), five are shifted upfield. The magnitudes of these shifts are very similar to the dinitrophenyl-induced ring-current shifts of the five tryptophan protons in the model Dnp-aspartate–tryptophan complex (Table 1). This suggests that the dinitrophenyl ring is stacked with a tryptophan residue in the combining site in a similar manner to that shown in the model system (Fig. 4).

If the dinitrophenyl and tryptophan form a charge-transfer pair in the Fv fragment, the relative orientation of the two residues should be very similar to that in the model compounds. An interaction of this nature would also be consistent with the extremely large quenching of the fluorescence of the Fv fragment on binding of Dnp- (or Tnp-) haptens. Reference to the model of Padlan *et al.* (1976) immediately suggests that it is tryptophan-93_L with which the dinitrophenyl ring must be interacting.

The upfield shifts of the dinitrophenyl protons when bound to the Fv fragment are far greater than those in the Dnp-aspartate–tryptophan complex, and are assumed to arise from ring-current interactions with additional aromatic residues. Inspection of tables of ring-current shifts shows that a minimum of two additional aromatic residues is required to explain the magnitude of the shifts.

Geometry of the combining site

The relative geometries of these aromatic rings can be obtained from an analysis of the ring-current data. For this analysis the distance of closest approach between any pair of aromatic rings was allowed for by including on the ring-current contour maps the van der Waals surfaces of the interacting molecules.

Fig. 12 shows a structure consistent with the observed shifts. In addition to the tryptophan residue parallel to the dinitrophenyl, a second aromatic residue above, and in van der Waals contact with, the $H_{(5)}$ and $H_{(6)}$ protons of the dinitrophenyl is sufficient to account for the shifts on these protons. A third aromatic residue is required to account for the shift on the $H_{(3)}$ proton, but here, with one reference point, it is only possible to define the relative geometry to within 0.04 nm. There are other constraints that help to fix the relative geometry of this ring with respect to the dinitrophenyl ring (see below). The ring-current shifts from each ring are summarized in Table 3.

This structure is also consistent with the small

Table 3. *Comparison of the predicted and observed ring-current shifts (in p.p.m.) in the combining site of protein MOPC 315 on addition of Dnp-aspartate based on the structure in Fig.* 13

Ring giving rise to shifts ...		Predicted shifts (p.p.m.) Dnp	Trp	A	B	Total	Obs.†
Dnp	$H_{(3)}$		0.79	0.80	0.12	1.7	1.68
	$H_{(5)}$		0.45	0.17	1.7	2.3	2.3
	$H_{(6)}$		0.38	0.08	0.87	1.35	1.31
Trp	$H_{(2)}$	0.1				0.1	0.19
	$H_{(4)}$	0.3				0.3	0.26
	$H_{(5)}$	0.23				0.23	† 0.18
	$H_{(6)}$	0.27				0.27	0.18
	$H_{(7)}$	0.5				0.5	0.26
A*	$H_{(2)}$	−0.06				−0.06	
	$H_{(3)}$	−0.05				−0.05	−0.3
	$H_{(4)}$	−0.06				−0.06	−0.3
	$H_{(5)}$	−0.1				−0.1	−0.1
	$H_{(6)}$	−0.2				−0.2	
B*	$H_{(2)}$	−0.09				−0.09	†
	$H_{(3)}$	−0.13				−0.13	
	$H_{(4)}$	−0.09				−0.09	
	$H_{(5)}$	−0.1				−0.1	
	$H_{(6)}$	−0.15				−0.15	

* These rings are as labelled in Fig. 12.

† The protein shifts have not been assigned to particular protons.

Table 4. *Change in chemical shift of hapten resonances perturbed on binding of haptens to the Fv fragment from protein MOPC* 315
Measurements were made at 270 MHz, T=303 K, in the presence of 0.15 M-NaCl.

Hapten	Proton	Shift change (p.p.m.)	pH*
Dnp-L-aspartate	$H_{(3)}$	1.68	6.9
	$H_{(5)}$	2.30	
	$H_{(6)}$	1.30	
	β-CH_2-	0.16	
Dnp-glycine	$H_{(3)}$	1.21	6.8
	$H_{(5)}$	2.20	
	$H_{(6)}$	1.77	
	α-CH_2-	1.00	
Dnp-O^-	$H_{(3)}$	1.25	6.7
	$H_{(5)}$	2.00	
	$H_{(6)}$	1.15	

Table 5. *Random-coil positions of aromatic protons in protein high-resolution n.m.r. spectra*
Resonance positions are measured with respect to the sodium salt of 3-(trimethylsilyl)propanesulphonic acid as external standard.

Amino acid	No. of carbon-bound protons	Expected multiplet structure*	No. of protons	Shift (p.p.m.)
Histidine	2	Two singlets	1, 1	~8.8–7.8†
				~7.6–7.2
Tyrosine	4	Two doublets	2, 2	6.9, 7.2
Phenylalanine	5	One triplet	1	
		One doublet	2	7.4
		One triplet		
Tryptophan	5	One singlet	1	7.3
		Two doublets	1, 1	7.7, 7.5
		Two triplets	1, 1	7.2, 7.3

* The multiplet structure will in general not be resolved for any of the resonances in proteins the size of fragment Fv.
† The $C_{(2)}$ and $C_{(4)}$ resonances of histidine move upfield with increasing pH.

shifts observed for the protein resonances on addition of hapten (Table 2). Other types of structure, for example those involving only two aromatic rings, are not consistent with these data. Although Fig. 12 uses the structure of the dinitrophenyl–tryptophan complex shown in Fig. 4, one of the rings is rotated through 180°, which is permissible because of the plane of symmetry for the indole ring (see the Appendix). This structure anticipates the results obtained and discussed below for the hapten side chain of Dnp-glycine and on the orientation of the indole side chain in the combining site.

Finally we note that the fully bound shifts of the hapten protons are independent of pH in the range 5–9, which means that the geometry of the combining site and the mode of hapten binding are unaltered over this pH range.

Binding of Dnp-O^- and Dnp-glycine to the Fv fragment

The changes in the resonance positions of protons in the Fv fragment and of the hapten resonances were monitored at 270 MHz by carrying out titrations with Dnp-O^- and Dnp-glycine similar to that described in detail above for the binding of Dnp-aspartate to the Fv fragment. The results for the hapten resonances are given in Table 4. The shifts on the dinitrophenyl proton resonances are very similar for the two haptens, suggesting that they are bound in similar ways to the Fv fragment despite two or three orders of magnitude difference in their affinity constants for the Fv fragment.

The side-chain CH_2 protons of Dnp-glycine experience a shift of about 1 p.p.m. on binding to the Fv fragment. (This shift is the average of that on the two

protons.) On the basis of the arrangement of the three aromatic rings shown in Fig. 12, the expected shifts on the CH_2 group of this hapten would be less than 0.5p.p.m. upfield. It is therefore necessary to introduce a fourth aromatic amino acid residue to account for the total observed shift on the CH_2 protons. An aromatic ring approx. 0.35nm away would give the necessary contribution of 0.5p.p.m.

Second layer of aromatic amino acid residues in the combining site

Further information on the aromatic nature of the combining site is obtained by comparing the initial resonance positions and intensities of the aromatic protons of the Fv fragment which are perturbed on hapten binding (Table 2) with the resonance positions and intensities expected for the aromatic protons in random-coil positions (Table 5). Thus the initial resonance positions (i.e. in the absence of hapten) at 6.62, 6.37, 6.33 and 6.16p.p.m. (Table 2) (a total of seven protons) are significantly ring-current-shifted upfield, irrespective of whether they originate from tryptophan, phenylalanine or tyrosine residues. The magnitudes of these shifts, approx. 1p.p.m., are such that these protons must be approx. 0.3nm above the plane of the neighbouring aromatic residues giving rise to these ring-current interactions. Reference to Fig. 12 and the use of ring-current tables each indicates that none of the three aromatic residues of the combining site shown interacts sufficiently to alter the expected resonance positions of any of the others significantly.

The seven proton resonances discussed above presumably come from some of these aromatic residues. To explain the initial upfield positions of the perturbed resonances, it is necessary to have a minimum of a further three aromatic rings which can interact with them. This leads to the concept of a second layer of aromatic residues around the combining site (Fig. 7). With this high density of aromatic residues in and around the combining site and the extreme sensitivity of ring-current shifts to small relative movements, the very few protons perturbed on hapten binding provide further confirmation that any conformational changes on hapten binding are extremely small.

Use of the Overhauser effect to provide additional refinement of residue positions in the combining site

A much shorter range effect than that of ring currents arises from the dipolar interactions between nuclei. If we consider two resonances A and B from nuclei which are very close in space, then applying a radio frequency field to resonance A will result in a change in the integrated intensity of B. This phenomenon has a $1/r^6$ dependence, and is termed the Overhauser effect (Noggle & Schirmer, 1971). In practice such effects are observed only if the nuclei are less than 0.3nm apart.

Fig. 13 shows the spectrum of a mixture of the Fv fragment and Dnp-O^- in 1:4 molar ratio. It also shows the effect on the intensity of the $H_{(3)}$ resonance caused by irradiation of the spectrum at various positions. At each irradiation position the spectrum

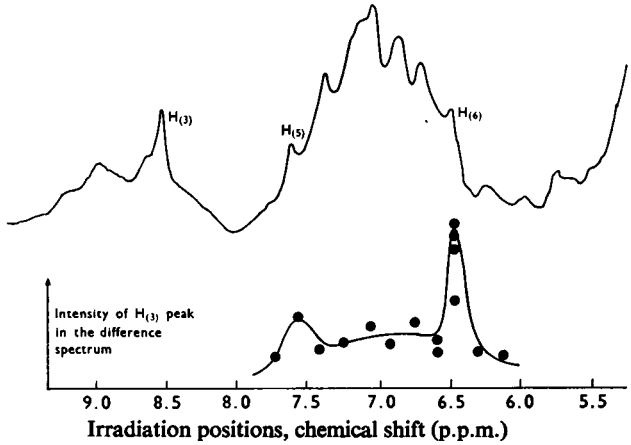

Fig. 13. *Intensity of the nuclear Overhauser effect at 270MHz on the $H_{(3)}$ proton resonance of the dinitrophenyl ring as a function of the irradiation position*

The aromatic region of the n.m.r. spectrum of the Fv fragment and Dnp-O^-, showing the effect on the $H_{(3)}$ resonance caused by irradiation at various positions. The greater the Overhauser effect the greater the intensity of the $H_{(3)}$ peak in the difference spectrum. The positions of the $H_{(5)}$ and $H_{(6)}$ resonances of the hapten are also indicated. The ratio of Fv fragment/Dnp-O^- is 1:4, pH6.7, T=303K; the solutions contained 0.15M-NaCl.

is subtracted from a blank (irradiating well outside the protein region as a control for instrumental effects, etc.), and the resulting intensity of the peak in the difference spectrum is then plotted against the irradiation position. Despite some variations between successive determinations reflecting the critical experimental conditions, the results show clearly that an Overhauser effect occurs between the $H_{(3)}$ proton and a resonance at 6.6p.p.m.

Similar, but less extensive, experiments were carried out with solutions of Dnp-aspartate and the Fv fragment. Irradiation at approx. 6.6p.p.m. also caused a significant diminution in intensity (approx. 30%) of the $H_{(3)}$ proton on the dinitrophenyl ring. This is expected, since the ring-current shifts (Table 3) indicate that the modes of binding of these two haptens are very similar. Thus the resonance at approx. 6.6p.p.m. causing the Overhauser effect on the $H_{(3)}$ proton arises from the same proton in each case.

The relative geometry of the $H_{(3)}$ proton and the aromatic ring (A) (Fig. 12) is already fixed quite accurately by the ring-current-shift data. The requirement from the Overhauser results, that the aromatic proton at 6.6p.p.m. is within 0.3nm of the $H_{(3)}$ proton, is met by moving the aromatic ring (A) below the $H_{(3)}$ proton into van der Waals contact with the dinitrophenyl ring.

Combining site of the Fv fragment of protein MOPC 315: a comparison of n.m.r. data with model-building studies

To a first approximation there is excellent agreement between the predicted combining site (Fig. 7) based on model-building studies of Padlan *et al.* (1976) and the experimental results. The outstanding feature of the model is a double layer of aromatic residues which surrounds the dinitrophenyl ring. Because of the proximity of these rings to one another and the sensitivity of ring-current shifts to the position of nearby aromatic residues, n.m.r. provides the means of positioning the first layer accurately to within 0.1nm. Thus it is possible to conclude from the n.m.r. studies that the orientation of the indole side chain of tryptophan-93_L must be in such a position that several of its protons can experience ring-current shifts from the second layer of aromatic residues. This is possible only if tryptophan-93_L points back into the site where some of the protons on the six-membered ring of the indole can be upfield-shifted by phenylalanine-98_L. Location of the dinitrophenyl ring to overlap with tryptophan-93_L in this position also gives a binding depth of 1.1–1.2nm, in agreement with e.s.r. (Dwek *et al.*, 1975*a*,*b*) and other determinations (Valentine & Green, 1967; Wilder *et al.*, 1975).

Reference to the model also allows the aromatic residues on the Fv fragment interacting with the hapten aromatic protons to be assigned to tyrosine-34_L and phenylalanine-34_H, whereas the aromatic amino acid residue responsible for the shift on the CH_2 protons of Dnp-glycine can only be tyrosine-33_L. This latter point is extremely important, for it effectively fixes the hapten orientation within the site. For the CH_2 protons of Dnp-glycine to be ring-current-shifted significantly by tyrosine-33_H, the hapten must be positioned so that phenylalanine-34_H is above the $H_{(5)}$ and $H_{(6)}$ protons of the dinitrophenyl ring and the $H_{(3)}$ protons must be over tyrosine-34_L.

Two corollaries now follow. First, since there is an Overhauser effect on the dinitrophenyl $H_{(3)}$ proton from a protein proton, this must be from tyrosine-34_L. This protein resonance, at 6.6p.p.m., is itself ring-current-shifted and so there must be a further aromatic residue interacting with tyrosine-34_L. We have already suggested that leucine-103_H should be repositioned so that its side chain projects away from the site. This would mean that tyrosine-104_H must be repositioned to point into the edge of the site. This allows closer approach of tyrosine-104_H and tyrosine-34_L, enabling them to cause a ring-current shift of each other's resonances.

The second corollary concerns the possible hydrogen-bonding scheme. The presence of two nitro groups on the hapten, which appear to be necessary for strong binding, suggests some hydrogen-bonding to amino acid side chains (Haselkorn *et al.*, 1974). Positioning of one or more of the protons of tyrosine-34_L within 0.3nm of the $H_{(3)}$ proton and yet maintaining the ring-current contribution of tyrosine-34_L to the $H_{(3)}$ proton shift results in tyrosine-34_L coming into contact with the dinitrophenyl van der Waals surface. The middle of the tyrosine-34_L ring is then below either the $C_{(2)}$ or $C_{(4)}$ atoms of the dinitrophenyl ring. Ring-current calculations cannot distinguish between these two possibilities. However, if the middle of the tyrosine-34_L ring is below the $C_{(4)}$ atom of the dinitrophenyl ring, the hydroxyl group is then in a position to bond to the 2-nitro group of the dinitrophenyl ring. The positioning of the hapten from the n.m.r. results also places the 4-nitro group in a position to hydrogen-bond to asparagine-36_L. It is noteworthy that both groups are on the light chain, and the observation that the light chain itself binds dinitrophenyl (Schecter *et al.*, 1976) may be a consequence of this. The n.m.r. data thus suggest a unique mode of hapten binding, and the positioning of the residues from the data provide a functional sense to the model-building studies of Padlan *et al.* (1976). The refined model of the combining-site residues based on the data in this paper is shown in Fig. 14.

The positions of the aromatic rings around the binding site are estimated to be accurate to ± 0.05nm, if it is assumed that the aromatic rings are the only source of upfield shifts, and that there is no motional

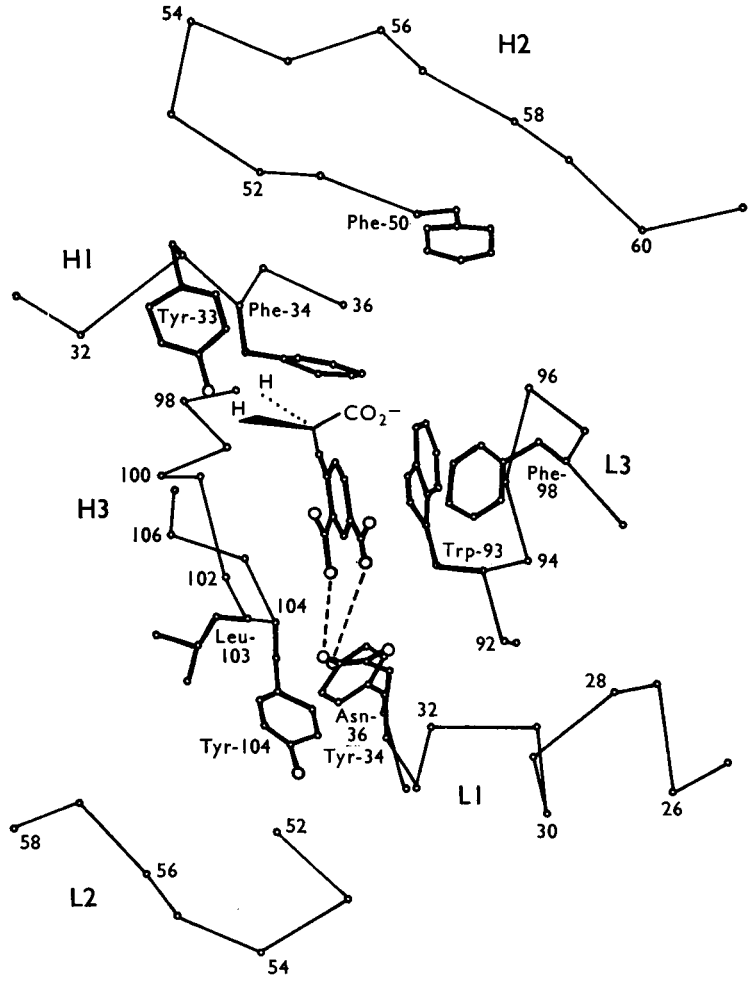

Fig. 14. *Refined combining site of protein MOPC* 315

This is based on the n.m.r. data presented in this paper. The positions of phenylalanine-34_H, tyrosine-34_L, tryptophan-93_L and tyrosine-33_H are obtained from the ring-current calculations. Tyrosine-104_H can interact with tyrosine-34_L. Some of the second layer of aromatic residues is shown. Thus the orientation of the hapten is such that the two nitro groups can form hydrogen bonds to asparagine-36_L and tyrosine-34_L.

averaging of these rings. We are, however, aware that there could be other factors contributing to the observed shifts of the hapten proton resonances. In particular, anisotropy effects of carbonyl groups and electrostatic effects may be important. However, such effects tend to be rather small and extremely localized, as shown by the work on lysozyme (Campbell *et al.*, 1975*b*). More importantly, all the carbonyl groups in the combining site (those of leucine-92_L, tyrosine-33_H, asparagine-101_H and leucine-103_H) are more than 0.4nm from any of the Dnp-hapten protons. Since the contribution from such carbonyl groups to the chemical shift of the hapten protons would be very much less than 0.1 p.p.m. (Jackman & Sternhell, 1969), we feel justified in neglecting them as an important factor in accounting for the observed shifts.

One final point concerns the lengths of the possible hydrogen bonds indicated in Fig. 14. That involving asparagine-34_L has a length of 0.4nm and that involving tyrosine-34_L is 0.24nm. Positioning the hapten so that the hydrogen bonds are about equal in length (about 0.3nm, which is typical of the hydrogen-bond distances normally observed), and yet maintaining the restrictions on the relative geometries of the aromatic rings imposed by the ring-current shifts and the Overhauser effect, requires two

conditions: (1) phenylalanine-34_H has to rotate through 0.04nm away from tyrosine-33_H, and (2) the 2-nitro group of the hapten has to be distorted by 30°. These modifications to the combining site (Fig. 14) may be an attractive possibility, since this movement of the phenylalanine-34_H would preclude the side chain of asparagine-99_H from participating in the site, a point that has worried Padlan *et al.* (1976). Further analysis on other haptens will help to distinguish these different possibilities for hydrogen-bonding.

Antibody–hapten reaction is a single association step

In n.m.r., the exchange rate $(1/\tau)$ is identified with the dissociation rate constant k_{off}. For intermediate exchange, $k_{off} \approx 2\pi\Delta\omega$, where $\Delta\omega$ is the change in chemical shift in Hz. On binding of Dnp-aspartate to the Fv fragment, the $H_{(5)}$ resonance shows some broadening. This effect is maximal when about 50% of the dinitrophenyl is bound, indicating that $H_{(5)}$ is in intermediate exchange. Thus, from the above relationship, the shift of 2.3p.p.m. ($3900s^{-1}$) for the $H_{(5)}$ resonance gives an estimate for k_{off}. This value of k_{off}, together with the measured binding constant, allows k_{on} to be calculated as approx. $2\times10^8 s^{-1}$. This is of the same order as the values obtained by Haselkorn *et al.* (1974) for a variety of Dnp-haptens, and is typical of bimolecular diffusion-controlled reactions. The n.m.r. results thus support the idea of Haselkorn *et al.* (1974) that the antibody–hapten reaction can be visualized as a single association step in which the dinitrophenyl ring enters the site and immediately senses the aromatic environment as manifested by the ring-current shifts on the hapten.

Effect of hapten binding on local mobility of residues in the combining site

The difference spectra in Fig. 6 show that there are more resonances in the positive than in the negative in the aromatic region. As we noted in Table 2, certain aromatic resonances in the Fv fragment are broadened out on the addition of hapten. A possible mechanism for such broadening is exchange, in which resonances experience a variety of environments with different chemical shifts. The resulting 'uncertainty' in the chemical shift can result in broad resonances, and the broadening will depend on the rate at which these environments are sampled. The most likely source of line broadening of aromatic residues in proteins comes from exchange involving either phenylalanine or tyrosine residues. The work of Campbell *et al.* (1975*a*) has shown that both these residues can flip rapidly about their axes of symmetry. This makes the two *ortho* (and the two *meta*) proton resonances equivalent. The rates of flipping are 10^3–$10^4 s^{-1}$, and, if the motion becomes less rapid, or if the chemical-shift difference between the *ortho* (or *meta*) environments is increased, severe broadening could result. In the Fv fragment, the small shifts on the protein resulting from hapten binding suggest that the broadening results from the hapten altering the rate of flipping of the nearby tyrosine or phenylalanine residues.

Conclusion on the specificity of protein MOPC 315 for dinitrophenyl ligands

The results of the studies in this paper support the use of model building to predict the combining sites of immunoglobulins. The predicted properties of the binding site of protein MOPC 315 based on the assumption of framework invariance are in good agreement with the experimental results.

The dinitrophenyl ring forms a stacking complex with tryptophan-93_L, and, this interaction, when occurring in an 'aromatic box' of tryptophan-93_L, phenylalanine-34_H and tyrosine-34_L, results in highly favourable contributions to the free energy of binding. There is also the possibility of enthalpy contributions from hydrogen bonds involving the two nitro groups and asparagine-36_L and tyrosine-34_L. The binding-energy contributions from the dinitrophenyl side chains may reflect their transfer into the non-polar site. This is illustrated by comparing the affinity of Dnp-O^- (approx. 1mM) with Dnp-aspartate or Dnp-glycine (approx. 10μM). The n.m.r. studies show that in each case the dinitrophenyl ring binds in a very similar manner. The difference in affinity reflects mainly the substitution with the neutral NH in Dnp-aspartate for the charged $-O^-$ of Dnp-O^-. Additionally in haptens carrying charged tail groups there is the possibility of electrostatic interactions with the charged groups at the entrance of the site (aspartate-101_H, lysine-52_H, arginine-95_L and histidine-102_H).

We thank Professor R. R. Porter, F.R.S., for his encouragement, many suggestions and support in this problem. We have all benefited from the interest and advice of Professor D. C. Phillips, F.R.S., Professor R. J. P. Williams, F.R.S., and Miss Elizabeth Press. We thank the M.R.C. and S.R.C. for financial support. We also thank Dr. D. Davies for kindly providing the co-ordinates for Fig. 7 before publication. R. A. D. is a member of the Oxford Enzyme Group. D. G. is the recipient of an EMBO short-term fellowship.

References

Amzel, L. M., Chen, B. L., Phizackerley, R. P., Poljak, R. J. & Saul, F. (1974) *Prog. Immunol. Proc. Int. Congr. Immunol. 2nd* **1**, 85–92

Campbell, I. D., Dobson, C. M. & Williams, R. J. P. (1975*a*) *Proc. R. Soc. London Ser. A* **345**, 41–59

Campbell, I. D., Dobson, C. M. & Williams, R. J. P. (1975*b*) *Proc. R. Soc. London Ser. A* **345**, 485–502

Davies, D. R., Padlan, E. A. & Segal, D. M. (1975*a*) *Contemp. Top. Mol. Immunol.* **4**, 127–155

Davies, D. R., Padlan, E. A. & Segal, D. M. (1975*b*) *Annu. Rev. Biochem.* **44**, 639–667

Dwek, R. A. (1973) *Nuclear Magnetic Resonance in Biochemistry*, Clarendon Press, Oxford
Dwek, R. A., Knott, J. C. A., Marsh, D., McLaughlin, A. C., Press, E. M., Price, N. C. & White, A. I. (1975*a*) *Eur. J. Biochem.* **53**, 25–39
Dwek, R. A., Jones, R., Marsh, D., McLaughlin, A. C., Press, E. M., Price, N. C. & White, A. I. (1975*b*) *Philos. Trans. R. Soc. London Ser. B* **272**, 53–74
Dwek, R. A., Givol, D., Jones, R., McLaughlin, A. C., Wain-Hobson, S., White, A. I. & Wright, C. E. (1976) *Biochem. J.* **155**, 37–53
Eisen, H. N., Simms, E. S. & Potter, M. (1968) *Biochemistry* **7**, 4126–4134
Epp, O., Colman, P., Fehlhammer, H., Bode, W., Schiffer, M., Huber, R. & Palm, W. (1974) *Eur. J. Biochem.* **45**, 513–524
Freed, R. M., Rockey, J. H. & Davis, R. C. (1976) *Immunochemistry* **13**, 509–515
Gartland, G. L., Freeman, C. R. & Bugg, C. E. (1974) *Acta Crystallogr. B* **30**, 1841–1849
Givol, D. (1974) *Essays Biochem.* **10**, 73–103
Hanson, A. W. (1964) *Acta Crystallogr.* **17**, 559–568
Haselkorn, D., Friedman, S., Givol, D. & Pecht, I. (1974) *Biochemistry* **13**, 2210–2222
Hochman, J., Inbar, D. & Givol, D. (1973) *Biochemistry* **12**, 1130–1135
Inbar, D., Hochman, J. & Givol, D. (1972) *Proc. Natl. Acad. Sci. U.S.A.* **69**, 2659–2662
Jackman, L. M. & Sternhell, S. (1969) *Nuclear Magnetic Resonance Spectroscopy in Organic Chemistry*, pp. 88–92, Pergamon Press, Oxford
Johnson, C. E. & Bovey, F. A. (1958) *J. Chem. Phys.* **24**, 1012–1014
Johnston, M. F. M., Barisas, B. G. & Sturtevant, J. M. (1974) *Biochemistry* **13**, 390–396
Little, J. R. & Eisen, H. N. (1967) *Biochemistry* **6**, 3119–3125
Noggle, J. H. & Schirmer, R. E. (1971) *The Nuclear Overhauser Effect*, Academic Press, New York
Padlan, E. A., Davies, D. R., Pecht, I., Givol, D. & Wright, C. E. (1976) *Cold Spring Harbor Symp. Quant. Biol.* **41**, in the press
Poljak, R. J. (1975) *Adv. Immunol.* **21**, 1–33
Poljak, R. J., Amzel, L. M., Chen, B. L., Phizackerley, R. P. & Saul, F. (1973) *Proc. Natl. Acad. Sci. U.S.A.* **70**, 3305–3320
Poljak, R. J., Amzel, L. M., Chen, B. L., Phizackerley, R. P. & Saul, F. (1974) *Proc. Natl. Acad. Sci. U.S.A.* **71**, 3440–3444
Rockey, J. H., Montgomery, P. C., Underdown, B. J. & Dorrington, K. J. (1972) *Biochemistry* **11**, 3172–3181
Schecter, I., Ziv, E. & Licht, A. (1976) *Biochemistry* **15**, 2785–2790
Schiffer, M., Girling, R. L., Ely, K. R. & Edmundson, A. B. (1973) *Biochemistry* **12**, 4620–4631
Segal, D. M., Padlan, E. A., Cohen, G. H., Rudikoff, S., Potter, M. & Davies, D. R. (1974) *Proc. Natl. Acad. Sci. U.S.A.* **71**, 4298–4302
Valentine, R. C. & Green, N. M. (1967) *J. Mol. Biol.* **27**, 615–617
Wain-Hobson, S., Dower, S. K., Gettins, P., Givol, D., Mclaughlin, A. C., Pecht, I., Sunderland, C. & Dwek, R. A. (1977) *Biochem. J.* **165**, 227–235
Wilder, R. L., Green, G. & Schumaker, V. N. (1975) *Immunochemistry* **12**, 55–60

APPENDIX

Application of Ring-Current Theory Based on the Johnson–Bovey Equation to the Aromatic Amino Acids

By S. J. PERKINS,* S. K. DOWER,† P. GETTINS,† S. WAIN-HOBSON† and R. A. DWEK†
Laboratory of Molecular Biophysics, Department of Zoology, University of Oxford, South Parks Road, Oxford OX1 3PS, U.K., and †Department of Biochemistry, University of Oxford, South Parks Road, Oxford OX1 3QU, U.K.

The calculation of the ring-current shifts was by the semi-classical Johnson–Bovey (1958) equation:

$$\delta' \times 10^{-6} = \left(\frac{ne^2}{6\pi mc^2 a}\right)\left\{\frac{1}{[(1+\rho)^2+z^2)^{\frac{1}{2}}]}\right\}\left\{K+\left[\frac{(1-\rho^2-z^2)}{(1-\rho)^2+z^2}\right]E\right\} \quad (1)$$

in e.s.u., where ρ is the chemical-shift difference in p.p.m. between the benzene signal and a close olefinic analogue, n is the number of electrons, a is the current-ring radius, e, m and c are the standard constants, K and E are the first and second complete elliptic integrals, and are a function of ρ, z and q, where q is the separation of the aromatic ring from the π-electron cloud and ρ and z are the radial and elevational cylindrical co-ordinates respectively (all three being in units of a).

The equation is derived by considering the secondary magnetic field produced by two currents of electrons, at distances $\pm q$ above and below the aromatic-ring atomic plane. The classical equations for the current and for the magnetic field are used.

When the biochemical application of the Johnson–Bovey (1958) equation is considered, due account must be made of the arbitrary aspects that arise from the theory's semi-classical nature. Accordingly, in its application to tryptophan, phenylalanine, tyrosine